UCLA
UCLA Electronic Theses and Dissertations

Title
The Development of Real-time Endocytic Monitoring using Bioluminescent Nanocapsules and Quantification Models

Permalink
https://escholarship.org/uc/item/3974t5gn

Author
Castillo, Roxanne

Publication Date
2020

Peer reviewed|Thesis/dissertation

eScholarship.org Powered by the California Digital Library
University of California

UNIVERSITY OF CALIFORNIA

Los Angeles

The Development of Real-time Endocytic Monitoring using Bioluminescent Nanocapsules and Quantification Models

A thesis submitted in partial satisfaction

of the requirements for the degree Master of Science

in Chemical Engineering

by

Roxanne Castillo

2020

© Copyright by

Roxanne Castillo

2020

ABSTARCT OF THE THESIS

The Development of Real-time Endocytic Monitoring
using Bioluminescent Nanocapsules and Quantification Models

by

Roxanne Castillo

Master of Science in Chemical Engineering
University of California, Los Angeles, 2020
Professor Yunfeng Lu, Chair

The transport of substances across the membrane and into the cell is essential for homeostasis. While biomolecules are intracellularly transported for essential functions of cellular growth and disposal, novel delivery vectors utilize the processes of endocytosis for therapy treatment, disease diagnosis, gene editing, and more. The use of fluorescent-based technologies to examine the kinetics of transported substances limits the quantification of the dynamic events occurring in endocytosis. Herein, the development of a tool to monitor the endocytic process in real-time using bioluminescent nanocapsules and quantification models is assessed. In the context of cervical cancer cells undergoing treatment, the platform introduces the potential of novel parameters in the development of optimal delivery vector design and in the development of drug treatments.

The thesis of Roxanne Castillo is approved.

Samanvaya Srivastava

Junyoung O. Park

Yunfeng Lu, Committee Chair

University of California, Los Angeles

2020

Dedication

I dedicate this work to my family. My family has taught me the value of hard work, dedication, and passion. Because of their support and encouragement, I have the opportunity to expand my skillset as a critical thinker and explore my passion for science.

Table of Contents

List of Figures

List of Tables

Acknowledgements

I thank Dr. Lu for his support and guidance in the development of this project. I thank all Lu Lab members for their continued support and encouragement. Learning with them all has molded me into the scientist I am today.

I thank Dr. Srivastava and Dr. Park for being on my committee and reviewing this work.

I thank Springer Nature for the permission to use the illustration of the endocytic pathway in Figure 1 in this work.

This material is based upon work supported by the National Science Foundation Graduate Research Fellowship Program.

1 Introduction

The transport of substances across the cellular membrane and into the cell is essential to homeostasis[1]. Transported substances into the cell vary from nutrients needed for cellular growth and function to unwanted pathogens for degradation and disposal. In the time of robust innovation in biotechnology, the intracellular delivery of biomolecules is a growing field with a growing demand. Scientists continue to develop novel carrier-systems to deliver biomolecules into the cell for treatment therapy[2], disease diagnosis[3], gene editing[4], and more[5]. While research in the development and applications of intracellular delivery vehicles is prominent, limitations in the rational design of delivery vehicles may exist due to the lack of advanced and accessible technology capable of quantifying the dynamic cellular processes of endocytosis.

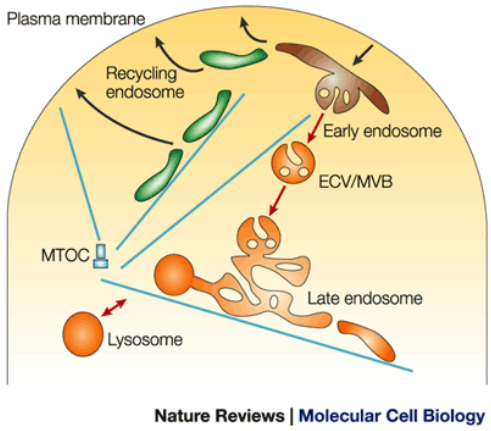

Figure 1. Outline of the endocytic pathway. From "The endocytic pathway: a mosaic of domains," by J. Gruenberg, 2001, *Nat Rev Mol Cell Biol*, *2*(10), p.721-730. Copyright 2019 by Springer Nature.

The endocytic processes in a cell are dynamic and depending on the internalized molecule, can be very complex. Briefly, at the beginning of the internalization process the plasma membrane

interacts with the macromolecule of interest, invaginates and pinches off, forming an endocytic vesicle[6]. The macromolecule is then delivered to an early endosome where the macromolecule is efficiently sorted for recycle or degradation[7], as outlined in Figure 1 (Gruenberg, 2001, p.722). If a macromolecule cannot escape the endocytic pathway and is determined not recyclable, the early endosome matures into a late endosome where the internal pH decreases, starting the degradation process[8]. Finally, the late endosome further matures by combining with synthesized lysosomal hydrolases to ultimately fuse with a lysosome, a point-of-no-return[9].

Unwarranted changes in cellular endocytic processing have been associated with certain health disorders while naturally occurring changes in endocytic processing due to common cellular events are of current interest. For example, the impaired acidification of lysosomes and reduced lysosomal hydrolysis are associated in patients with a class of mutations in Parkinson's disease. The inability of lysosomes to acidify accelerates the development of Parkinson's disease-like neuropathology[10]. In the context of natural cellular events, when stimulated with an apoptosis-inducing agent, a gradual increase in lysosomal pH was observed[11]. While research in endocytic processes is under development, the need for better, dynamic tools to investigate the complex dynamics of endocytosis remains.

The current tools to investigate the endocytic processes of a cell are limited and influence the information known about the complex processes of cellular endocytosis. Traditional and accessible methods of analyzing endocytosis include fluorescent microscopy[12] and flow cytometry[13]. While the area of fluorophores is continually developing to include innovative systems such as sensors for the measuring metal ions in living systems[14] and the screening of HIV protease activity in cells[15], fluorescent detection methods are limiting in the information they offer in that fluorescent data is discrete, semi-quantitative, sometimes ambiguous, and often requires

pre-treatments involving many steps. Specifically, the necessary treatment before analysis of fluorescent samples forces the discrete nature of fluorescent data rather than an in real-time measurement. Equally, the arbitrary fluorescent units of fluorescent data make it difficult to form an accurate quantification of cellular events. Further, accessible methods often leave the physical position of a fluorophore open to interpretation. Colocalization techniques can determine the overlap between two entities but fluorescent techniques often require additional modifications to ensure an entity presents itself within the cell or on the exterior surface.

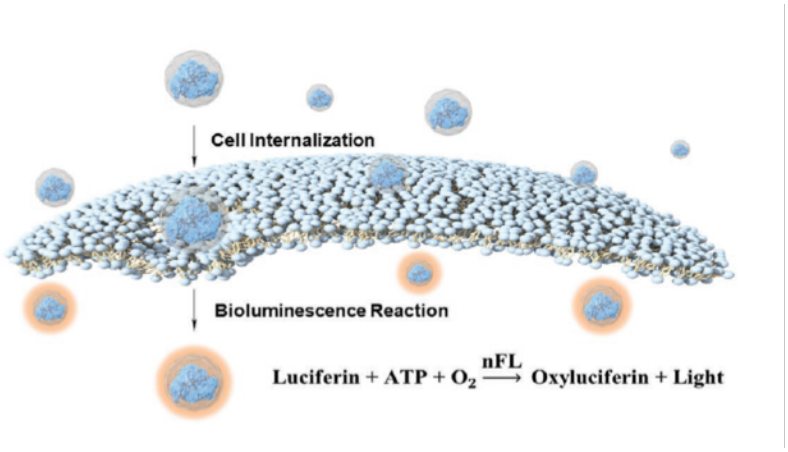

Figure 2. A schematic of the internalization of encapsulated Firefly Luciferase (nFL) that catalyzes the bioluminescent reaction of luciferin in the presence of cytosolic ATP.

Herein, the development of a tool for real-time endocytic monitoring using bioluminescent nanocapsules and quantification models is discussed. Taking advantage of the presence of ATP in copious amounts in the cytosol[16,17] and minimal amounts in extracellular environment[18,19], encapsulated Firefly Luciferase luminesces upon cellular entrance, effectively allowing the modeling of its bioluminescent reaction to monitor endocytic processes in real-time and quantify the key events of endocytosis. As detailed in Figure 2 above, encapsulated Firefly Luciferase

interacts with the cellular membrane, is engulfed, and luminesces in the presences of the substrates of Firefly Luciferase in the cytosol. The real-time bioluminescent rate is then recorded and modeled to provide a quantification of endocytic events, serving as a complementary tool to the limitations of current fluorescent technologies. In this work, the extent of the platform is developed, characterized, and explored in the context of induced apoptosis in cervical cancer cells using a common chemotherapeutic treatment.

2 Materials and Methods

2.1 Materials

All chemicals and materials were purchased from Sigma-Aldrich and used as recommended, unless otherwise stated. Recombinant Escherichia coli (E. coli) expressing Firefly Luciferase was purchased from Excellgen. LB medium was purchased from Apex Bioresearch Products. The nickel-resin, HisPur Ni-NTA, was purchased from Thermo Scientific. Luciferin potassium salt was purchased from Gold Biotechnology. Cell Titer Blue cell viability assay kit was purchased from Promega Corporation. HeLa cells were purchased from American Type Culture Collection (ATCC). Dulbecco's Modified Eagle Medium (DMEM) growth medium, 0.25% Trypsin and Penicillin-Streptomycin were purchased from GenClone. Fetal Bovine Serum (FBS) was obtained from Corning. Paclitaxel was obtained from Aladdin Industrial Corporation.

2.2 Instruments

UV-Visible spectra were acquired with a NanoDrop One (Thermo Scientific). Dynamic light scattering (DLS) and Zeta Potential studies was performed on a Zetasizer Nano (Malvern Instruments Ltd., Kingdom). Transmission electron microscopy (TEM) images were obtained on T12 Quick CryoEM and CryoET (FEI). Bioluminescence intensities and absorbance were measured with a Tecan Infinite 200 PRO plate reader. Flow cytometry was performed with a MACSQuant Analyzer (Miltenyi Biotec). Cells were maintained in a Heracell VIOS 160i CO2 Incubator (Thermo Scientific) and routinely checked with an automated cell counter, Countess I (Invitrogen).

2.3 Extraction of Firefly Luciferase from Bacteria

Firefly Luciferase was produced and extracted in-house. Briefly, his-tagged Firefly Luciferase was expressed in bacteria, purified using immobilized metal affinity chromatography and assessed for enzymatic activity, protein concentration, and protein purity as detailed below.

2.3.1. Expression in E coli

Recombinant Firefly Luciferase was produced and purified from bacterial cells. Once transformed in *E. Coli* Rosetta2, the cells were grown in LB medium (25 g/L) supplemented with kanamycin (50 g/mL), held a temperature of 37 °C, and shaken at 170 rpm. Once mature at an OD600 of 0.8, the *E.coli* were induced to express Firefly Luciferase by adding isopropyl -D-thiogalactoside (IPTG) at a final concentration of 1 mM. To protect the enzymatic activity of the Firefly Luciferase, the temperature was kept at 16 °C for the 24-hour induction period. After induction, the cells were harvested by centrifugation (5300 rpm) for 10 min and resuspended in Purification Buffer (200 mM NaCl, 50 mM NaH_2PO_4, pH 7.4). To effectively extract the protein, phenylmethylsulfonyl fluoride (PMSF) was added at a final concentration of 1μM and the cells were lysed via sonication in intervals for 15 min. To remove the cell debris, the sonicated solution was centrifuged at 17,000 rpm for 90 min and passed through a 0.22 μm vacuum filter.

To purify the Firefly Luciferase from the other proteins, a Ni-NTA gravity column was used. The column was first equilibrated with Purification Buffer. The extracted protein was then passed through the column and washed with 10 column volumes of Purification Buffer then 10 column volumes of each Washing Buffer. Twenty millimolar, 40 mM, 60 mM imidazole in Purification Buffer were used as each Washing Buffer in ascending order. To finally elute the his-

tagged Firefly Luciferase, 250 mM imidazole in Purification Buffer was used as the eluant and the enzymatic activity of the elution was monitored using the protocol in the following section**.** To remove the excess imidazole for the future use of the enzyme, the protein was dialyzed 6 times against PBS for 3 days. The protein was later stored in aliquots at -80 °C. To protect the activity of the protein throughout the purification process, all materials were prechilled at 4 °C.

2.3.2. Enzymatic Activity

The rate of the bioluminescent reaction of Firefly Luciferase was monitored to quantify the activity of the purified protein. To prepare for the activity assay, a Substrate Buffer was made consisting of 20 mM tricine, 3.74 mM magnesium sulfate ($MgSO_4$), 0.1 mM ethylenediaminetetraacetic acid (EDTA), and 2 mM dithiothreitol (DTT) in DI water and adjusting the pH to 7.4. The Substrate Buffer was then supplemented to make the complete Activity Buffer by adding 27 μL of Coenzyme A solution (CoA, 10mM in DI water), 10.6 μL of adenosine triphosphate solution (ATP, 50 mM in PBS), and 47 μL of D-Luciferin solution (10 mM in PBS) to 915.5 μL of Substrate Buffer solution. To perform the activity assay, 2 μL of the Firefly Luciferase sample were added to 35 μL of Activity Buffer in a 96-well plate. The bioluminescent intensity was quickly measured using a luminometer set with an exposure time of 1 second.

2.3.3. Protein Concentration

The Bicinchoninic Acid (BCA) assay was used to determine the protein concentration of the extracted solutions. A series of stock solutions were prepared as the standard in concentrations

of 0, 0.5, 1.0, and 2.0 mg/mL of Bovine Serum Albumin (BSA). The reacting mixture was prepared by adding BCA Reagent B to BCA Reagent A from the Pierce BCA Protein Assay Kit in a 1:50 ratio. Then, each sample of standard and unknown was prepared by adding 100 µL of DI water, 100 µL of the reacting mixture containing BCA Reagent A and B, and 5 µl of sample and placing the samples in a water bath at 60 °C for 30 minutes. Sixty microliters of each sample were then placed in a 96-well plate in triplicate and the absorbance at 562 nm was measured using a spectrophotometer. The unknown concentration values were then calculated via linear regression analysis.

2.3.4. Protein Purity

To assess the purity of the produced, purified enzyme an SDS-PAGE was utilized. To prepare, a separating gel consisting of 10% acrylamide and stacking gel of 4% acrylamide was made. The samples of firefly luciferase were mixed with equal volumes of Loading Buffer (25% glycerol, 2.5% sodium dodecyl sulfate, 0.01% *w/v* bromophenol blue, 100 mM fresh dithiothreitol in 125 mM Tris-Cl, pH 6.8) and loaded in the wells of a freshly made SDS-PAGE in parallel with a protein ladder. The gel was then run at 300V and 45 mA until the free-dye indicator in the Loading Buffer ran out of the gel. The SDS-PAGE was then removed from the glass sandwich and placed in Fixing Buffer (50% *v/v* ethanol, 10% *v/v* acetic acid in DI water) for an hour to immobilize the separated proteins. The gel is then placed in Staining Buffer (0.5 mg/ml Coomassie Brilliant Blue, 50% *v/v* ethanol, 10% *v/v* acetic acid in DI water) for at least an hour. After removing the excess stain in deionized water or De-staining Buffer (25% *v/v* ethanol, 5% *v/v* acetic acid in DI water) the pigmented bands were compared to known controls and analyzed for purity.

2.4 Synthesis of Encapsulated Firefly Luciferase

To enhance the stability in experimentation and penetrability of Firefly Luciferase across the cell membrane, the protein was encapsulated according to previous methods[20] with slight modification.

2.4.1. In situ Polymerization

To prepare for the *in situ* polymerization, monomer stock solutions consisting of acrylamide (AAM, 30% *m/v*) and N-(3-aminopropyl) methacrylamide (APM, 20% *m/v*) were made. To crosslink the monomers, a solution of N,N'-methylenebisacrylamide (BIS, 10% *m/v*) was made in DMSO. Further, to protect the activity of the enzyme, adenosine triphosphate (ATP, 50 mM) and magnesium sulfate ($MgSO_4$, 100 mM) were prepared in PBS and DI water, respectively.

To begin the encapsulation process, a cocktail was made with ATP, $MgSO_4$, AAM, APM, and BIS according to Table 1 below along with 220 μL of PBS as diluting buffer. Then, the cocktail was added to 400 μL of a 2.7 mg/mL Firefly Luciferase solution, gently mixed by inversion, and initiated with 6 μL of ammonium persulfate (APS, 10% in DI water, *m/v*) and catalyzed with 7.9 μL of tetramethylethylenediamine (TEMED). The polymerizing solution was kept on ice for 1 hour until it was dialyzed against prechilled PBS to remove any unreacted reagents. To determine the encapsulated protein concentration after polymerization and dialysis, BCA Assay was used according to the section above. Encapsulated Firefly Luciferase, herein denoted as nFL, was kept on ice until further experimentation.

Component	Amount (µL)
ATP	42
$MgSO_4$	21
AAM	26
APM	7.5
BIS	16.2

Table 1. Cocktail solution of active site protectors, monomers, and crosslinkers for the encapsulation of Firefly Luciferase.

2.4.2. Nanocapsule Purification

To purify the nFL from its unencapsulated counterparts for characterization, an anion exchange column was used. Since the thin polymerized shell of AAM and APM around the protein increases the surface charge of the macromolecule in this platform, the unencapsulated protein retains its inherent negative charge and interacts with the cations in the exchange column while nFL does not. In detail, to prepare the sample for the Q Sepharose gravity flow column, the sample was transferred to a dilute buffer (20 mM PB) using an ultracentrifugation tube at 4000 rpm for 30 min. After equilibrating the column with 20 mM PB, the sample was loaded and let to flow through via gravity drip. To further elute the unbound nFL, more 20 mM PB was added and the elution was monitored in aliquots. The purified sample was then concentrated using an ultracentrifugation tube for further use. To clean the Q Sepharose column for future use, the column was washed with 2 column volumes of 2M NaCl, 4 column volumes of 1M NaOH, and again 2 column volumes of

2M NaCl. Finally, the column was washed with 2 column volumes of DI water and stored in DI water at 4 °C until further use.

2.5 Characterization of nFL

To characterize nFL, traditional methods of Transmission Electron Microscopy (TEM), Dynamic Light Scattering (DLS), and measuring the Zeta Potential (ZP) were used. To further characterize the potential of nFL in this platform, the catalytic characteristics, thermal and proteolytic stability, and cellular capabilities were studied as listed below.

2.5.1. Transmission Electron Microscopy

A Transmission Electron Microscope was used to examine the size and morphology of nFL. To prepare the sample, nFL was diluted to a concentration of 0.1 mg/mL, dipped on a carbon-coated copper grid, and let sit for 1-2 minutes. The sample was then removed from the grid, stained with uranium acetate (2% w/v) and incubated for another minute and a half. The uranium acetate was then removed, and the grid was let sit overnight until analyzed.

2.5.2. Dynamic Light Scattering & Zeta Potential

Dynamic Light Scattering was used to examine the hydrodynamic radius and size distribution of a sample while electrophoretic mobility was observed to measure the Zeta Potential of a sample. Encapsulated luciferase was suspended in 20 mM PB at a concentration of 1 mg/mL

and tested for size and surface charge using a Malvern Zetasizer. The number distribution was analyzed and compared to native Firefly Luciferase.

2.5.3. Enzymatic Characteristics

The Michaelis constant (K_M) and the turnover number (k_{cat}) were used in examining the catalytic characteristics of nFL and were essential in modeling the temporal bioluminescent rate. Similar to the activity buffer mentioned above, Coenzyme A (27 µL, 10 mM CoA in DI Water) and ATP (10.6 µL, 50 mM in PBS) were added to Substrate Buffer (915.5 µL). Forty-seven microliters of varying concentrations of Luciferin (0.625, 1.25, 2.5 5, 10 mM D-Luciferin in PBS) was added to prepare a series of activity buffers for analysis. Two microliters of nFL were then added to 35 µL of the activity buffers, recording the activity of nFL at each concentration of Luciferin. The recorded activity in Relative Light Units (RLU) in one second was then converted to the corresponding rate of bioluminescent reaction (mol of luciferin reacted) by a conversion factor ($3.90 \times 10^{11} \frac{RLU}{mol\ of\ oxyluciferin}$). A Lineweaver-Burk plot was then graphed using the reciprocal bioluminescent rate and the corresponding reciprocal Luciferin-substrate concentration. The x-intercept was then used to find K_M ($x_{int} = -\frac{1}{K_M}$) while the y-intercept was used to find k_{cat} ($y_{int} = \frac{1}{k_{cat} \cdot [E]}, [E] = total\ enzyme\ concentration$).

2.5.4. Thermal and Proteolytic Stability

The thermal and proteolytic stability of nFL and native Firefly Luciferase were assessed to observe the behavior of nFL in cellular-mimicking environments. The thermal stabilities were examined in PBS and Cell Growth Medium at 37 °C. In detail, the samples (0.4 mg/mL nFL or native FL) were added to warmed PBS or Cell Growth Medium (10% Fetal Bovine Serum, 1% Penicillin-Streptomycin in DMEM) and the activity of the sample was measured over the course of 45 minutes according to the Enzymatic Activity method listed above. Proteolytic stability was observed according to similar methods. The samples were added to a protease solution (0.1% Trypsin-EDTA in PBS) and the residual activity of the samples was recorded over the course of 45 minutes.

2.5.5. Cellular Penetrability

To assess the cellular penetrability of nFL, methods involving fluorescent flow cytometry were utilized to complement previous findings involving microscopy[20]. To prepare nFL for detection in flow cytometry, fluorescein isothiocyanate (FITC) was conjugated to APM monomers in the polymer shell of nFL. The labeling reagent (1% *w/v* FITC in DMSO) was added to the sample in a 1:3 molar nFL to FITC ratio. The pH of the reaction was adjusted to 8.0 (100 mM sodium bicarbonate buffer) and the reaction was let sit for 1 hour, protected from light. The sample was then dialyzed in PBS at least two times to remove any unconjugated labeling reagent and to exchange the sample to a physiological-suitable buffer. The concentration of the sample was measured using the BCA Assay and stored in 4 °C until further experimentation.

HeLa cells were raised and cultured as detailed below. Upon confluency, HeLa cells were seeded (~10^4 cells per well) in a 96-well plate and let sit for a day to properly adhere to the cell plate and reach a logarithmic-growth state. The cells were then treated with nFL for various incubation times. After the desired exposure to nFL, the nFL-containing medium was aspirated and the cells were gently rinsed with PBS to remove any remaining nFL and serum proteins. Each well was then treated with trypsin (0.25% Trypsin-EDTA) until the cells detached, resuspended in Complete Growth Medium, and fixed in paraformaldehyde (2.5 % Formalin). The fixed cells were then stored overnight in 4 °C until measured by the flow cytometer.

To assess the fluorescent intensity of nFL inside each individual cell, the 488 nm laser was used at appropriate voltages. To ensure fluorescent intensities were recorded from internalized nFL, a selective dye (0.095% *w/v* Trypan Blue) was used to quench the intensity of any nFL on the exterior of the cellular membrane. To begin the analysis, the forward scatter area (FSC-A) and forward scatter height (FSC-H) charts were scanned for singlets. To distinguish the intensities of the cells of interest from cellular debris, gates according to critical forward scatter area (FSC-A) and side scatter area (SSC-A) were utilized. Fluorescent Intensity Histograms and Median Fluorescent Intensities (MFI) values of the FITC conjugated nFL were then extracted from the data using FlowJo and the MFIs were statistically analyzed for differences using PRISM.

2.6 In-Vitro Preparation and Treatment

The growth and maintenance of the HeLa cell line were followed as advised by the American Type Culture Collection (ATCC). HeLa cells were grown in Complete Growth Medium (10% fetal bovine serum, 1% penicillin in DMEM) in an atmosphere of 95% air and 5% carbon

dioxide at 37 °C. The cells were passaged at no more than 80% confluency and routinely checked for membrane integrity using Trypan Blue (0.2% *m/v*).

2.6.1. In-Vitro Treatment

The endocytic process was monitored in apoptotic cells. To induce cellular apoptosis, HeLa cells were treated with varying concentrations of Paclitaxel (0.2, 2, 20, 200 nM in Complete Growth Medium), a chemotherapeutic treatment. Paclitaxel was dissolved in dimethyl sulfoxide (DMSO) as a concentrated stock and diluted in Complete Growth Medium so that a final concentration of DMSO would not exceed 0.1% (*v/v*). The plated HeLa cells were replaced with fresh medium carrying the chemotherapeutic treatment and observed for morphology under the microscope and cellular viability after 24 hours, using the methods listed below.

To determine the efficacy of the drug in inducing apoptosis and cell death, the Cell Titer Blue assay was used to determine cell viability. After desired treatment exposure, the treatment-carrying medium was aspirated and replaced with fresh Complete Growth Medium. Cell Titer Blue (0.025 mg/mL in Complete Growth Medium) was then added to each well and incubated for at least one hour at 37 °C to allow the conversion of the substrate. The converted substrate, indicative of the amount of metabolically active cells, was then measured using fluorescence at an excitation wavelength of 560 nm and an emission wavelength of 590 nm. Control wells treated with PBS in place of the anticancer drug were determined as 100% viable.

2.7 Real-Time Endocytic Monitoring using nFL and Quantitative Modeling

After determining critical anticancer concentrations in the HeLa cell line and observing the amount of internalized nFL from objective methods, bioluminescent nFL was used to monitor the cellular endocytic processes. Upon recording the bioluminescent rate over time, the data was modeled in MATLAB using the quantification models and used to extract various critical parameters.

2.7.1. Real-Time Endocytic Monitoring Assay using nFL

To monitor the endocytic process of nFL in real-time, HeLa cells were prepared as mentioned above. Briefly, HeLa cells were plated and let sit for a day. The cells were then replenished with fresh Cell Growth Medium carrying the desired treatment of Paclitaxel and incubated for 24 hours. Since the bioluminescent reaction of Firefly Luciferase needs the excited state of oxyluciferin to produce light, the HeLa cells were supplemented with luciferin (0.5 mg/mL in Complete Growth Medium) at the time of anticancer treatment.

After the incubation of HeLa with chemotherapeutic treatment and luciferin, the endocytic process was monitored in real-time using a plate reader. The nFL (0.4 mg/mL in Complete Growth Medium) was added to HeLa and the bioluminescence of each sample was measured with an exposure time of 1 second with no attenuation, every 30 seconds over the course of 3 hours. The rate of bioluminescent reaction (RLU/s) over time was then exported and analyzed in MATLAB using the quantifying models outlined above.

2.7.2. Cell Count

The number of HeLa cells per well recorded in the real-time measurement is critical in monitoring the endocytic process and obtaining the quantified amount of nFL internalized per cell. When preparing the cell plate for the Real-Time Endocytic Monitoring Assay, another cell plate is prepared and treated in parallel to accurately count the number of cells per well. The cells in the parallel plate are then removed from the treatment-carrying medium, gently rinsed with PBS, and treated with trypsin until all the cells in the well are detached. The cells are then fixed overnight in 1% paraformaldehyde at 4 °C and counted using the flow cytometer.

2.7.3. Quantitative Modeling

After recording the bioluminescent reaction rate over time, the data is modeled and parameters are extracted in MATLAB. To start, the recorded bioluminescence (RLU) of each well in one second over time is related to the concentration of nFL in a cell over time by the following Equation (1) model.

$$RLU = \frac{k_{cat}[S]}{K_M+[S]}[nFL]e^{-k_d t} \bullet A \bullet N \quad (1)$$

In detail, *N* is the number of cells per well as measured in the previous section, *A* is the conversion of RLU to moles of luciferin reacted, and k_d is the calculated decay constant of nFL. In detail, the previous conversion factor of light units to moles of luciferin was adjusted for the observed decrease in intensity. Since signals from within a cell are 68.422 times weaker than signals in lysed cells, an appropriate value for A was $5.93 \times 10^9 \frac{RLU}{mol\ of\ oxyluciferin}$ [21]. The variable, *[S]* signifies the luciferin substrate concentration, while K_M and k_{cat} are the calculated catalytic characteristics as

noted in an earlier section. As previously shown[20], substrate consumption of the endocytic process of nFL is estimated in the magnitude of nanomolar while the supplied substrate to the sample is in the magnitude of millimolar, making changes in substrate concentration insignificant throughout the process, and therefore constant. Similarly, ATP is also in excess since the reported cellular levels of ATP fall between 1-10 mM.

In order to define the concentration of nFL in the cell, the region of exponential-enzymatic decay was found and the decay constant was calculated. Upon taking the natural logarithm of Equation 1, a linear function of t is left as shown in Equation (2), below.

$$lnRLU = -k_d t + \ln\left(\frac{k_{cat}[S]}{K_M+[S]}[nFL] \bullet A \bullet N\right) \quad (2)$$

To extract the decay constant in MATLAB, the natural logarithm was taken of the values in bioluminescent rate over time curve and the most linear region was extracted. Taking the slope of that region supplied the model with the decay constant of the nFL, as previously reported.

After extracting the decay constant, the concentration profile of nFL over the time of the assay can be found. The rearranged Equation (3) is shown below.

$$[nFL] = \frac{RLU}{\frac{k_{cat}[S]}{K_M+[S]}[nFL]e^{-k_d t} \bullet A \bullet N} \quad (3)$$

2.7.4. Initial Rate of Uptake

To calculate the Initial Rate of Uptake (IRU), the linear portion of the beginning of the temporal nFL concentration curve was extracted and analyzed. Specifically, the first points of the graph were plotted and the segment was adjusted according to the linear correlation of the segment. To provide the best estimate of IRU, two squares of correlation were considered (r^2=0.95 and r^2=0.90). Points were added to the segment until the squares of correlation fell below the

considered values. The segment was then subject to a linear fit and the calculated slope was determined as the IRU.

2.7.5. Plateau Concentration

The Plateau Concentration ([$nFL_{plateau}$]) was determined by monitoring the standard deviation of the temporal nFL concentration profile. In detail, the standard deviation of 5 neighboring points was plotted against the corresponding index for the entire temporal concentration profile and compared to a threshold. When the standard deviation of 5 neighboring points fell below 10% of the maximum reported standard deviation, the index corresponding to the [$nFL_{plateau}$] was found.

3 Results and Discussion

3.1 Characterization of nFL

Once synthesized, nFL was characterized using traditional methods for morphology, size distribution, and surface charge. To start, the morphology was examined using TEM as shown in Figure 3A below.

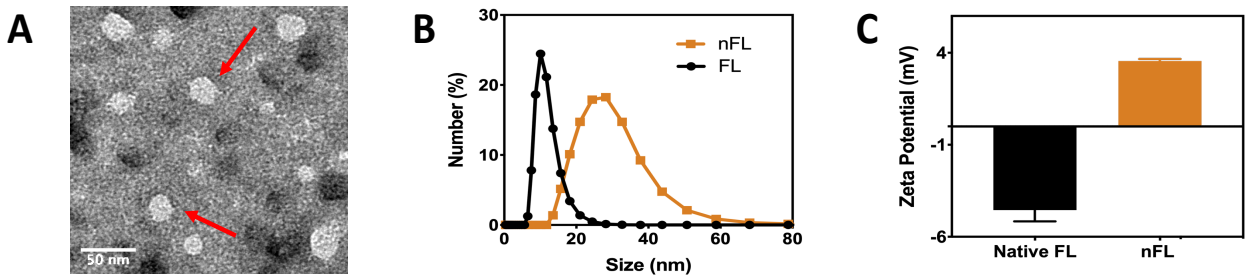

Figure 3. Characterization of nFL. A) A representative TEM image of nFL depicting spherical, uniform morphology. B) The size distribution of native Firefly Luciferase and nFL as measured by DLS. C) The surface charge of native Firefly Luciferase and nFL as determined by Zeta Potential.

As observed under TEM, nFL exhibit spherical morphology and uniform size distribution of 28.24 $\pm$1.52 nm in diameter. Upon further examination using DLS and Zeta Potential techniques, nFL exhibits notable changes in characteristics from its native counterparts. In Figure 3B, encapsulating Firefly Luciferase effectively increases the measured hydrodynamic size to 35 nm from 10 nm. The difference in size is owed to the growth of the thin polymer shell around the

individual proteins via free radical polymerization. Encapsulating Firefly Luciferase also effectively changes the surface charge of the protein as noted by the Zeta Potential. Dependent on the amount of APM present in the polymerization process, the surface charge of nFL increases linearly with the positive monomer to total monomer ratio. The ability to alter the monomer ratios involved in the polymerization process allows for the tunability of nFL for an array of applications. The specific recipe shown in Table 1 yields nFL with a positive surface charge of + 3.56 mV while native Firefly Luciferase remains at its inherent negative surface charge of – 4.55 mV as depicted in Figure 3C.

The spherical, uniform morphology and surface tunability of nFL make nFL an ideal candidate as an intracellular probe. Particles in the 20-30 nm range are reported to require the least energy to deform the cellular membrane during internalization[22], allowing for effective cellular penetration. Further, the slight positive charge of nFL increases its cellular penetration capabilities. It is theorized that the positive surface charge of particles readily interacts with the negatively charged cellular membrane, prompting the internalization of the particle[23].

3.2 Enzymatic Characterization of nFL

The enzymatic characteristics of nFL were observed to assess the compatibility of nFL as an in-vitro tool. As shown in Figure 4A, nFL luminesces only in the presence of the essential substrates of Firefly Luciferase. When the enzymatic system lacks ATP or Luciferin, nFL does not luminesce. The need for the presence of both substrates makes nFL a useful, accessible tool in observing the endocytic process. In detail, the compatibility of Luciferin in in-vitro assays is well studied. When using an in-vitro luciferase-based assay, Luciferin quickly diffuses into the cellular

environment and when given at appropriate doses, it has minimal toxicity[24]. Further, since cells have concentrations of 1-10 mM ATP in their cytosol, the bioluminescence of nFL should only occur once internalized. The positive charge of nFL allows it to interact with the negatively charged cell membrane to quickly translocate across the cellular membrane and luminesce where ATP presents itself, making nFL an ideal tool for monitoring the endocytic process.

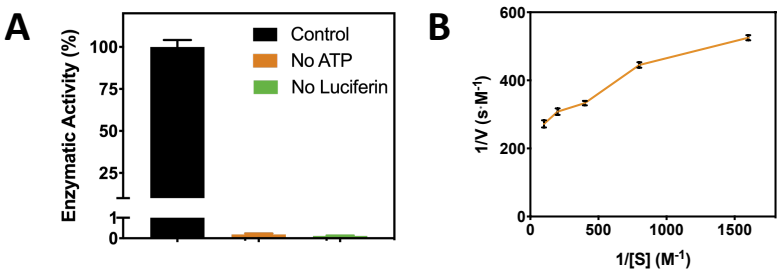

Figure 4. Enzymatic Characterization of nFL. A) The bioluminescent activity of nFL only luminesces in the presence of both ATP and Luciferin substrates. B) A representative Lineweaver-Burk plot of nFL was used to determine the Michaelis constant K_M turnover number k_{cat}.

The Michaelis constant (K_M) and the turnover number (k_{cat}) are essential in modeling the behavior of nFL in the cell. From Figure 4B it is noted that the nFL exhibits Michaelis-Menten kinetics. Values of K_M and k_{cat} were 6.2×10^{-4} M and 3273 s^{-1}, respectively, for a representative batch of nFL used in the monitoring of the cellular endocytic process. The low value of K_M suggests Luciferin and ATP quickly and effectively permeate the thin polymer shell of nFL while allowing nFL to be limited only by the internalization process, the variable of interest. The high value of k_{cat} highlights the quality of nFL as a robust tool. Once internalized, nFL quickly converts Luciferin to an excitable form using ATP. The quick accumulation of light units allows standard

plate readers to pick up on the catalyzed bioluminescent signal, making nFL a sensitive and reliable tool.

3.3 Thermal and Proteolytic Stability of nFL

The thermal and proteolytic stability of nFL were assessed to further quantify the capabilities of nFL as an in-vitro tool. To start, the thermal stability of nFL at 37 °C was assessed in PBS, a physiological-mimicking buffer, and Complete Growth Medium, the commonly found cellular environment in many in-vitro assays, as shown in Figure 5A and 5B.

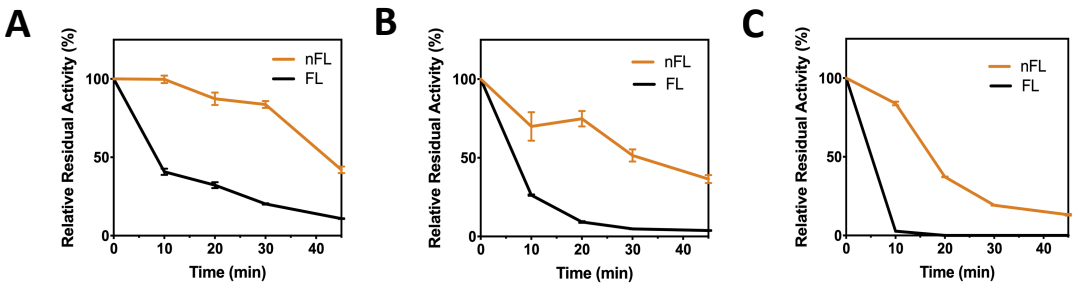

Figure 5. Thermal and Proteolytic Stability of native Firefly Luciferase and nFL. A & B) Thermal stability of Firefly Luciferase and nFL in A) PBS and B) Complete Growth Medium at 37 °C. C) Proteolytic stability of Firefly Luciferase and nFL in 0.1% trypsin at 37 °C.

The stability of nFL in PBS and Complete Growth Medium at 37 °C retains the activity of Firefly Luciferase better than the naked enzyme. In high-temperature environments, enzymes have the energy to transition to other conformational states that are often irreversible and detrimental to function. It is theorized that the thin polymer shell protects the internal enzyme by immobilizing

the essential physical conformation necessary for the active sites of the enzyme to remain functional.

As shown in Figure 5C, nFL surpasses naked Firefly Luciferase in activity retention in proteolytic environments. While the smaller byproducts of proteolysis may still permeate through, the encapsulating polymer net-like shell protects the internal enzyme from macromolecule substrates such as proteases. The immobilized conformation and physical encapsulating barrier can protect Firefly Luciferase against the harsh environments and proteases of endocytic processing, while still sensitizing it to provide tangible information about the endocytic process. While improvement in activity retention remains, nFL is a proven better tool than naked Firefly Luciferase in the monitoring of cellular endocytic processes.

3.4 Cellular Penetrability of nFL

To ultimately characterize nFL as an effective tool in the monitoring of cellular endocytic processes, the ability of nFL to cross the cellular membrane and luminesce was assessed. As depicted in Figure 6A and 6B, HeLa cells rapidly and continually internalize fluorescently labeled nFL under the chosen experimental conditions. The accumulation of nFL in under 10 minutes works well with the limited enzymatic window of nFL in cellular environments.

Given nFL can cross the cellular membrane in as little as 10 min, bioluminescent-functional nFL can cross the cellular membrane where Luciferin and ATP present themselves, and light up in a reporting fashion as depicted in Figure 6C. While cells introduced to native Firefly Luciferase also report bioluminescence in smaller magnitude and in a different rate profile, it is theorized that the internalization of nFL in a cell is rate-limiting. In other words, extracellular ATP

from natural cellular processes is more easily accessed than the intracellular ATP that is only accessible to nFL because of its morphology and surface charge. Unlike discrete data from flow cytometry, the temporal bioluminescent rate profile of nFL in a cell can be mathematically analyzed to a deeper extent to provide more information about the cellular endocytic process.

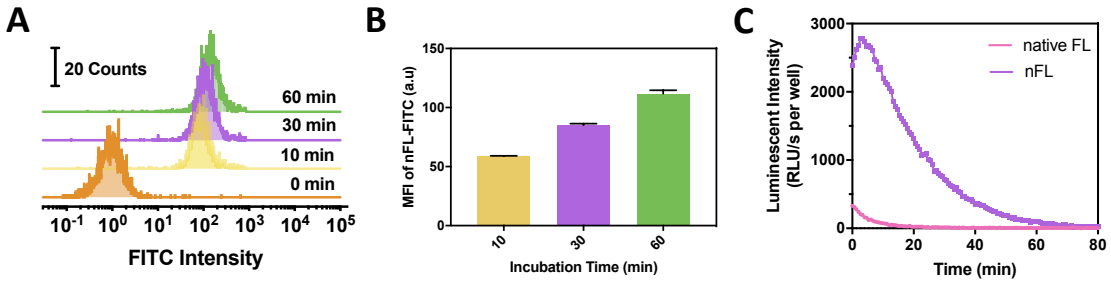

Figure 6. Cellular Penetrability of nFL. A) Flow Cytometry Histograms of HeLa cells treated with FITC conjugated nFL for 10 min, 30 min, and 60 min. B) Median-Fluorescent Intensities (MFI) of HeLa cell populations incubated with FITC conjugated nFL for 10 min, 30 min, and 60 min. C) The temporal bioluminescent rate profile of HeLa exposed to native Firefly Luciferase (FL) and nFL.

3.5 Accumulation of nFL in Apoptotic Cells

In search of finding differences in endocytic processing in cellular populations, the accumulation and bioluminescent rate of internalized nFL in apoptotic cells was assessed. When cells undergo natural or induced stresses, cells alter their systematic mechanisms and begin a form of programmed cell death known as apoptosis. To observe if endocytic processing is affected by apoptosis, HeLa cervical cancer cells were treated with varying concentrations of Paclitaxel. As a

traditional chemotherapeutic, Paclitaxel induces cellular apoptosis by halting cell division in quickly proliferating cells through microtubule inhibition. As noted in Figure 7A, HeLa cells treated with as little as 0.2 nM of Paclitaxel have a significant decreased cellular viability as reported from the Cell Titer Blue Assay. Though the Cell Titer Blue Assay in this experiment reports cell viability of over 50% in the HeLa cells treated with 200 nM Paclitaxel, future experiments include a negative control that should account for any previously converted substrate that serves as a background intensity in the sample.

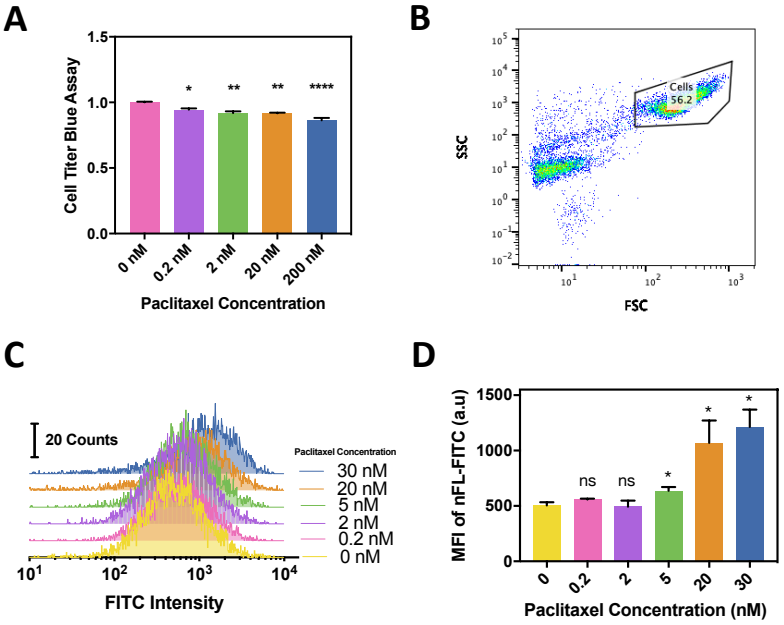

Figure 7. The accumulation of nFL in HeLa cells undergoing anticancer treatment. A) Cell viability of HeLa cells exposed to various concentrations of Paclitaxel for 24 hours. B) Representative gating of HeLa cells used in flow cytometry analysis. C) Flow Cytometry Histograms of Paclitaxel-treated HeLa cells incubated with FITC conjugated nFL for 1 hr. D) Median Fluorescent Intensities (MFI) of Paclitaxel-treated HeLa cell populations incubated with FITC conjugated nFL for 1 hr.

To assess the difference in the accumulation of nFL among apoptotic cells, HeLa cells treated with varying concentrations of Paclitaxel were incubated with fluorescently labeled nFL for an hour. The intensity of nFL was then measured using flow cytometry. To begin the analysis, gating of HeLa cells shown in Figure 7B was used to distinguish cells of interest from debris in the sample. Because the process of apoptosis is differential and cells exhibit different morphology throughout apoptosis, effectively affecting the side and forward scatter measurements, future experiments consider the use of apoptosis kits commonly used in flow cytometry to better distinguish the population of interest. Once gated, Flow Cytometry Histograms were graphed to visualize the difference in the accumulation of nFL among the treated samples as shown in Figure 7C. It is noted that distribution shifts to higher intensities of nFL as the concentration of treatment increases. The observation is further corroborated in analyzing the median fluorescent intensity (MFI) of the population, as graphed in Figure 7D.

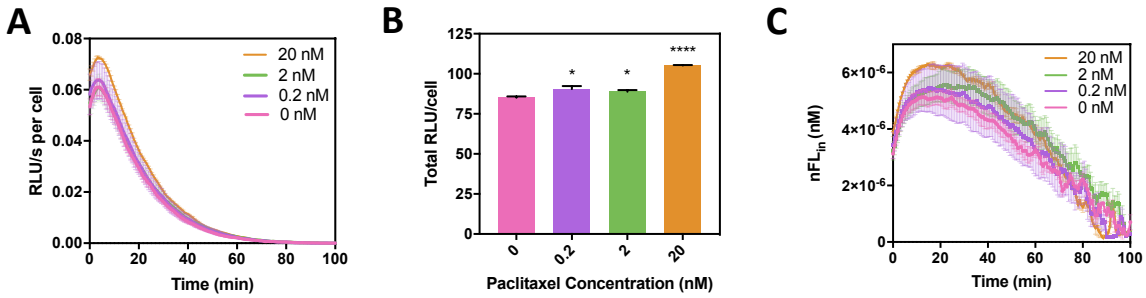

Figure 8. Real-time endocytic monitoring of HeLa cells undergoing anti-cancer treatment. A) The temporal bioluminescent rate profile of Paclitaxel-treated HeLa cells exposed to nFL. B) Average total bioluminescence emitted of a Paclitaxel-treated HeLa cell exposed to nFL for 100 min. C) The modeled temporal concentration profile of nFL in a Paclitaxel-treated HeLa cell.

To assess whether an endocytic monitoring tool using nFL is sensitive to the observations seen with flow cytometry, HeLa cells incubated with various concentrations of Paclitaxel were subject to nFL and the bioluminescent rate was monitored over time. Normalizing the sample to the number of cells present in a well, the average temporal bioluminescent rate profile per cell exposed to varying treatments is outlined in Figure 8A. A HeLa cell treated with the highest concentration of Paclitaxel exhibited a vertically shifted temporal rate profile compared to HeLa cells treated with less or no Paclitaxel. In further examination, the area under the average temporal bioluminescent rate profile per treated cell was calculated and statistically compared in Figure 8B. The data strongly corroborates observations found with the flow cytometer and since more total bioluminescent reactions occurred in cells treated with higher doses of Paclitaxel, the data suggest that cells undergoing anticancer treatment internalize more nFL and may better retain the enzymatic activity of nFL more than cells treated with less or no treatment. It is worth noting that the real-time endocytic monitoring tool using nFL detected differences in lower concentrations of Paclitaxel while flow cytometry did not.

Using the previously mentioned model, the temporal concentration profile of functional nFL is reported in Figure 8C. The concentration of functional nFL in a HeLa cell treated with 20 nM Paclitaxel is higher than those treated with less or no Paclitaxel in the first 40 minutes of endocytic monitoring as expected from the analysis with flow cytometry. The decay of the bioluminescence of nFL in HeLa cells treated with varying concentrations of Paclitaxel, among other parameters, appears to differ. Analyses of some parameters are noted below.

3.6 Differences in Parameters

After modeling the temporal bioluminescent rate profile to get the temporal concentration profile of bioluminescent nFL, three parameters were extracted from the concentration profile for analysis. To start, the plateau concentration of each curve was determined as recorded in Table 2 and compared statistically to the others as in Figure 9A. While it appears that the plateau concentration increases as treatment of Paclitaxel concentration increases, interestingly only the sample with the highest concentration was determined statistically significant. While initially it appears that the plateau concentration dataset contradicts our conclusions of the accumulation of nFL in treated cells using the flow cytometer, the bioluminescence of nFL can be sensitive to other parameters in the endocytic process. The sensitivity of nFL makes it a strong, dynamic tool with the potential to shed light on the dynamic processes of endocytosis and complement findings observed with flow cytometry.

Concentration of Paclitaxel (nM)	Plateau Concentration (nM)	Decay Constant (s^{-1})	IRU (nM/s)
0	4.88E-06	0.00091	3.21E-09
0.2	5.08E-06	0.00089	2.85E-09
2	5.05E-06	0.00092	2.65E-09
20	5.99E-06	0.00088	3.33E-09

Table 2. The parameters of Plateau Concentration, Decay Constant, and Initial Rate of Uptake extracted from the temporal concentration profile of nFL in HeLa cells treated with varying concentrations of Paclitaxel.

The decay constants of nFL in HeLa cells treated with varying concentrations of Paclitaxel were also explored and analyzed. While it appears that the decay constant is decreased in the sample treated with the highest concentration of Paclitaxel as recorded and graphed in Table 2 and Figure 9B, statistical analysis determined a p-value of 0.134. It is observed that the p-value does not meet traditional standards to determine a statistical difference, but it is acknowledged that future experiments should find sources of variation in the platform and include more points to strengthen the statistical analysis. Statistical differences in the decay constant of the sample treated with the highest concentration may shed information on the endocytic pathway such as the lack of acidification of lysosomes in apoptotic cells[11], potentially explaining the lack of differences in the plateau concentrations of the samples treated with 0.2 and 2 nM Paclitaxel.

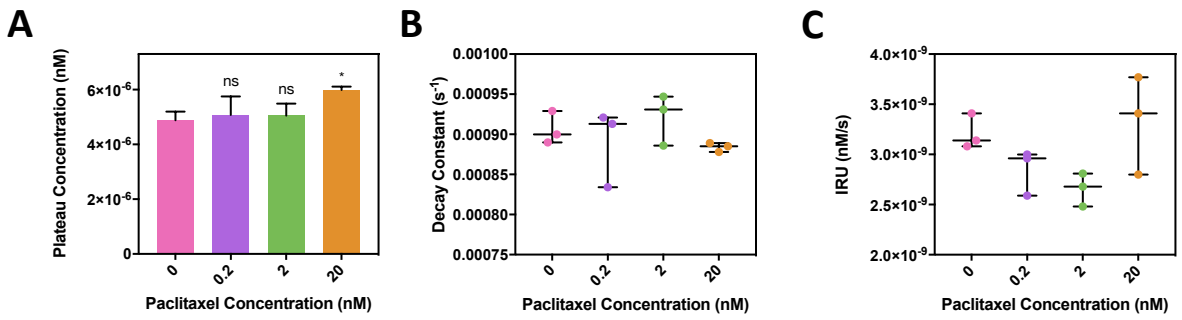

Figure 9. Extracted constants from the modeled temporal concentration profile of nFL in HeLa cells undergoing anticancer treatment. A) The Decay Constant of nFL in HeLa cells treated with various concentrations of Paclitaxel. B) The Plateau Concentration of nFL in HeLa cells treated with various concentrations of Paclitaxel. C) The Initial Rate of Uptake (IRU) of nFL in HeLa cells treated with various concentrations of Paclitaxel.

Similarly, limitations in making conclusions about the effect of treated Paclitaxel concentration on the Initial Rates of Uptake (IRU) in HeLa cells exist. While it initially appears that IRU is decreased as the concentration of treated Paclitaxel is increased, the IRU increases in the sample with the highest Paclitaxel treatment as noted in Figure 9C. It could be possible that paclitaxel differentially affects the extracted parameters of the temporal concentration profile of nFL in Hela cells, but large variations in the data and small sample size limit conclusions.

4 Conclusion

The use of bioluminescent nanocapsules as a quantifiable tool in real-time monitoring of endocytic processes has complemented the information offered from traditional and accessible fluorescent technologies. An increase in the accumulation of encapsulated luciferase in cervical cancer cells treated with a common anti-cancer treatment was observed using fluorescent methodologies. Using the developed real-time monitoring tool and quantification models, the observation of increased accumulation in treated cervical cancer cells was further corroborated while novel parameters were introduced. While further development is necessary to reach the potential of the platform, the introduction of novel parameters from real-time data such as Decay Constant, Plateau Concentration, and Initial Rate of Uptake provides an area of unexplored details in the processes of endocytosis. The unexplored details of endocytosis may be key to the development of optimal delivery vector design and the future of drug treatment development.

5 References

1. Patel, S., Kim, J., Herrera, M., Mukherjee, A., Kabanov, A. V., & Sahay, G. (2019). Brief update on endocytosis of nanomedicines. *Advanced Drug Delivery Reviews*, *144*, 90-111.

2. Gaston, J., Maestrali, N., Lalle, G., Gagnaire, M., Masiero, A., Dumas, B., ... & Berne, P. F. (2019). Intracellular delivery of therapeutic antibodies into specific cells using antibody-peptide fusions. *Scientific reports*, *9*(1), 1-12.

3. Ma, Y., Mao, G., Wu, G., Fan, J., He, Z., & Huang, W. (2020). A novel nano-beacon based on DNA functionalized QDs for intracellular telomerase activity monitoring. *Sensors and Actuators B: Chemical*, *304*, 127385.

4. Wei, T., Cheng, Q., Min, Y. L., Olson, E. N., & Siegwart, D. J. (2020). Systemic nanoparticle delivery of CRISPR-Cas9 ribonucleoproteins for effective tissue specific genome editing. *Nature communications*, *11*(1), 1-12.

5. Cao, Y., Chen, H., Qiu, R., Hanna, M., Ma, E., Hjort, M., ... & Melosh, N. A. (2018). Universal intracellular biomolecule delivery with precise dosage control. *Science advances*, *4*(10), eaat8131.

6. Alberts, B., Johnson, A., Lewis, J., Raff, M., Roberts, K., & Walter, P. (2002). Transport into the cell from the plasma membrane: endocytosis. In *Molecular Biology of the Cell. 4th edition*. Garland Science.

7. Gruenberg, J. (2001). The endocytic pathway: a mosaic of domains. *Nature reviews Molecular cell biology*, *2*(10), 721-730.

8. Cooper GM. The Cell: A Molecular Approach. 2nd edition. Sunderland (MA): Sinauer Associates; 2000. Lysosomes.

9. Huotari, J., & Helenius, A. (2011). Endosome maturation. *The EMBO journal*, *30*(17), 3481–3500.

10. Colacurcio, D. J., & Nixon, R. A. (2016). Disorders of lysosomal acidification—the emerging role of v-ATPase in aging and neurodegenerative disease. *Ageing research reviews*, *32*, 75-88.

11. Wang, X., Fan, L., Zhang, X., Zan, Q., Dong, W., Shuang, S., & Dong, C. (2020). A red-emission fluorescent probe for visual monitoring of lysosomal pH changes during mitophagy and cell apoptosis. *Analyst*, *145*(21), 7018-7024.

12. Michalet, X., Kapanidis, A. N., Laurence, T., Pinaud, F., Doose, S., Pflughoefft, M., & Weiss, S. (2003). The power and prospects of fluorescence microscopies and spectroscopies. *Annual review of biophysics and biomolecular structure*, *32*(1), 161-182.

13. Braun, G. B., Friman, T., Pang, H. B., Pallaoro, A., De Mendoza, T. H., Willmore, A. M. A., ... & Reich, N. O. (2014). Etchable plasmonic nanoparticle probes to image and quantify cellular internalization. *Nature materials*, *13*(9), 904-911.

14. Carter, K. P., Young, A. M., & Palmer, A. E. (2014). Fluorescent sensors for measuring metal ions in living systems. *Chemical reviews*, *114*(8), 4564-4601.

15. Ai H. W. (2014). Fluorescent sensors for biological applications. Sensors (Basel, Switzerland), 14(9), 17829–17831.

16. Mo, R., Jiang, T., DiSanto, R., Tai, W., & Gu, Z. (2014). ATP-triggered anticancer drug delivery. *Nature communications*, *5*(1), 1-10.

17. Leist, M., Single, B., Castoldi, A. F., Kühnle, S., & Nicotera, P. (1997). Intracellular adenosine triphosphate (ATP) concentration: a switch in the decision between apoptosis and necrosis. *The Journal of experimental medicine*, *185*(8), 1481-1486.

18. Traut, T. W. (1994). Physiological concentrations of purines and pyrimidines. *Molecular and cellular biochemistry*, *140*(1), 1-22.

19. Gorman, M. W., Feigl, E. O., & Buffington, C. W. (2007). Human plasma ATP concentration. *Clinical chemistry*, *53*(2), 318-325.

20. Wu, D., Yang, Y., Xu, P., Xu, D., Liu, Y., Castillo, R., ... & Qin, M. (2019). Real-Time Quantification of Cell Internalization Kinetics by Functionalized Bioluminescent Nanoprobes. Advanced Materials, 31(39), 1902469.

21. Ignowski, J. M., & Schaffer, D. V. (2004). Kinetic analysis and modeling of firefly luciferase as a quantitative reporter gene in live mammalian cells. Biotechnology and bioengineering, 86(7), 827-834.

22. Zhang, S., Li, J., Lykotrafitis, G., Bao, G., & Suresh, S. (2009). Size-dependent endocytosis of nanoparticles. Advanced materials, 21(4), 419-424.

23. Liu, J., Zhang, R., & Xu, Z. P. (2019). Nanoparticle-based nanomedicines to promote cancer immunotherapy: Recent advances and future directions. Small, 15(32), 1900262.

24. Yeh, H. W., Karmach, O., Ji, A., Carter, D., Martins-Green, M. M., & Ai, H. W. (2017). Red-shifted luciferase–luciferin pairs for enhanced bioluminescence imaging. Nature methods, 14(10), 971.